Available at
www.ElsevierComputerScience.com
POWERED BY SCIENCE DIRECT

Signal Processing 84 (2004) 1895–1908

SIGNAL PROCESSING

www.elsevier.com/locate/sigpro

Improved initialization for time domain equalization in ADSL

Katleen Van Acker[a], Geert Leus[b,1], Marc Moonen[c,*], Thierry Pollet[a]

[a]Alactel Bell, Access to Networks, Corporate Research Center, Francis Wellesplein 1, 2018 Antwerpen, Belgium
[b]Faculty of Electrical Engineering, Mathematics, and Computer Science, Delft University of Technology, Mekelweg 4, 2628 CD Delft, The Netherlands
[c]Department of Electrical Engineering (ESAT), Katholieke Universiteit Leuven, Kasteelpark Arenberg 10, 3001 Leuven, Belgium

Received 11 March 2001; received in revised form 21 June 2004

Abstract

An improved optimization algorithm for the time domain equalizer (TEQ) is developed for discrete multitone (DMT) based asymmetric digital subscriber line (ADSL). In contrast with existing algorithms, our algorithm explicitly disregards the unused tones in the cost function as well as in the non-triviality constraint. Simulation results are presented for the upstream channel. It is shown that the achievable bitrate is higher than for a popular existing algorithm.

Keywords: Discrete multitone; Equalization; ADSL

1. Introduction

Equalization is required in a DMT-system to combat intercarrier and intersymbol interference [10]. Basically, the equalization relies on the insertion of a cyclic prefix and a 1-tap frequency domain equalizer. However, when the order of the channel impulse response is larger than the cyclic prefix length, interferences arise. Hence, additional equalization techniques are called for. Mostly time domain equalization to shorten the channel impulse response is then adopted [2–9,13–16].

Minimum mean-square error (MMSE) channel shortening is a well-known time domain equalizer design approach. The cost function is quadratic and has a unique minimum, which leads to low-complexity

*Corresponding author. ESAT/SISTA, Katholieke Universiteit Leuven, Kasteelpark Arenberg 10, 3001 Heverlee, Belguim. Tel.: +32-1632-1927; fax: +32-1632-1970.

E-mail addresses: katleen.van_acker@alcatel.be (K. Van Acker), leus@cas.et.tudelft.nl (G. Leus), marc.moonen@esat.kuleuven.ac.be (M. Moonen), thierry.pollet@alcatel.be (T. Pollet).

[1]Also for correspondence.

0165-1684/$ - see front matter
doi:10.1016/j.sigpro.2004.06.014

algorithms. To avoid the trivial zero solution, the minimization is subject to a certain non-triviality constraint. Although this design procedure is very popular, it has some important disadvantages resulting from the fact that MMSE channel shortening is not equivalent to bit rate optimization.

To improve the performance of MMSE channel shortening, we propose a new algorithm called *weighted MMSE channel shortening*. It differs from previously presented algorithms in that the unused tones are explicitly disregarded in the cost function as well as in the non-triviality constraint, by introducing weight matrices. This weighted MMSE channel shortening is still not equivalent to bit rate optimization, but it comes close. Note that many tones are labeled as unused from the outset because they overlap the plain old telephone service (POTS) band, or because they are used for the other direction in case of frequency division duplexing (FDD) systems, or because they occupy a band that is used for radio amateurs.

A more advanced equalizer structure can be obtained by shifting the time domain equalizer to the frequency domain. By optimizing this equalizer for each tone separately, we can then obtain true bit rate optimization, as discussed in [12]. Although this so-called per tone equalizer is simple to implement, it is difficult to design, needs a lot of memory, and requires an adaptation of the current modem architectures. Therefore, we want to stick to cheap time domain equalizer design in this paper.

In Section 2, we give a comprehensive review of MMSE channel shortening and formulate the main disadvantages. We then introduce weighted MMSE channel shortening in Section 3. Simulation results are given in Section 4 and show that weighted MMSE channel shortening significantly outperforms classical MMSE channel shortening in the upstream direction. Finally, conclusions are drawn in Section 5.

Notation: Upper (lower) bold face letters denote matrices (column vectors); frequency-domain components are indicated by a tilde; $(\cdot)^{\mathrm{T}}$, $(\cdot)^{*}$ and $(\cdot)^{\mathrm{H}}$ denote transpose, complex conjugate, and complex conjugate transpose (or Hermitian), respectively; $\mathscr{E}\{\cdot\}$ represents the statistical expectation; $\|\cdot\|$ represents the Frobenius norm and $|\cdot|$ the absolute value; $\mathbf{I}_N$ denotes the $N \times N$ identity matrix and $\mathbf{0}_{M\times N}$ the $M \times N$ all-zero matrix; diag$\{\mathbf{x}\}$ represents the diagonal matrix with the vector $\mathbf{x}$ on the diagonal and diag$\{\mathbf{X}\}$ the diagonal matrix with the main diagonal of the matrix $\mathbf{X}$ on the diagonal; $\otimes$ denotes the Kronecker product; and finally, to select an element, subvector, or submatrix from a vector or matrix we use Matlab notation.

2. MMSE channel shortening

A DMT system avoids intercarrier and intersymbol interference if a cyclic prefix with sufficient length is added to each transmitted symbol. More specifically, the prefix length has to be equal to or longer than the order L of the channel impulse response (CIR) $\mathbf{h} = [h_0, \ldots, h_L]^{\mathrm{T}}$. Hence, it results in a minimal efficiency loss of $L/(N+L)$, with N the DMT symbol size. For ADSL, this minimal efficiency loss would be unacceptably high.

Typically, a T-tap time domain equalizer (TEQ) is therefore introduced before demodulation (e.g., in ADSL with $T = 32$ for the downstream and $T = 64$ for the upstream) to equalize the CIR to a shorter target impulse response (TIR) such that it ‘fits’ into a given cyclic prefix length v. The efficiency loss then decreases to $v/(N+v)$.

Several algorithms are proposed in literature [2–9,13–16] that search for a T-tap TEQ $\mathbf{w} = [w_0, \ldots, w_{T-1}]^{\mathrm{T}}$, such that its convolution with the CIR $\mathbf{h}$ is closest to an arbitrary TIR of order v, denoted by $\mathbf{b} = [b_0, \ldots, b_v]^{\mathrm{T}}$. The basic MMSE channel shortening approach is shown in Fig. 1. One searches for a TEQ $\mathbf{w}$, a TIR $\mathbf{b}$, and a decision delay δ_{tot}, such that the following cost function is minimized:

$$J = \mathscr{E}\{e_l^2\} = \mathscr{E}\{([y_l, \ldots, y_{l-T+1}]\mathbf{w} - [x_{l-\delta_{\mathrm{tot}}}, \ldots, x_{l-\delta_{\mathrm{tot}}-v}]\mathbf{b})^2\}, \tag{1}$$

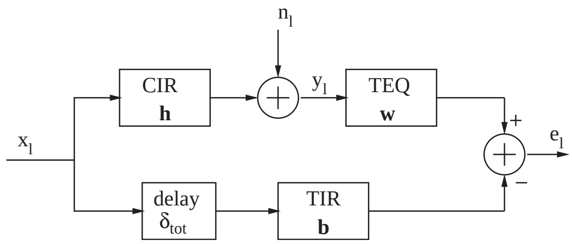

Fig. 1. TEQ design by MMSE channel shortening.

where y_l and x_l are the output and input signal, respectively, with l the sample index. Note that δ_{tot} is the 'total' decision delay introduced by the channel and can be written as $\delta + \delta_0 - 1$, where the reference delay δ_0 indicates the first sample of the maximal energy interval of length $v + 1$ in $\mathbf{h}$, and δ denotes the 'relative' decision delay under consideration. To avoid trivial solutions (i.e., zero vectors $\mathbf{w}$ and $\mathbf{b}$), a non-triviality constraint is applied, which can be a unit norm, unit tap, or unit output energy constraint on either $\mathbf{w}$ or $\mathbf{b}$ [17].

Shortening the channel impulse response by means of a MMSE criterion has no direct relation to the optimal bit rate, which results in unsatisfactory performance. The non-triviality constraint also has no relation to the bit rate, and hence it may be difficult to select the appropriate constraint. Besides the non-optimal capacity, another aspect of the unsatisfactory behavior of the MMSE shortening algorithm is the non-smoothness of the resulting bit rate as a function of the decision delay. Hence, an optimal delay is not easily selected beforehand, and an exhaustive search over a large range of delays is needed during modem initialization.

3. Weighted MMSE channel shortening

In an attempt to improve the performance of the shortening algorithm, we modify the cost function as well as the non-triviality constraint. Unlike [14], our algorithm explicitly disregards the unused tones in the cost function and the non-triviality constraint, which is achieved by introducing weight matrices. The constrained optimization problem still is quadratic and has a unique minimum. Note that this approach is not equivalent to bit rate optimization as is performed by the geometric TEQ [1], which leads to a nonlinear optimization problem, in general without a unique minimum.

In the sequel, we first derive the new cost function and non-triviality constraint. We then interpret the resulting constrained optimization problem. Finally, we discuss how to compute the required correlation matrices. Thereby, we first assume the additive channel noise and input signal are white, and then show how these expressions extend when we want to take the noise and input color into account.

3.1. Cost function

Our aim is to take into account the DMT nature in the cost function. Therefore, we have to develop a cost function on the DMT symbol level and need to sum (1) over $l = \delta_{\text{tot}}, \ldots, \delta_{\text{tot}} + N - 1$. Hence, the new cost function becomes

$$J = \mathscr{E}\{\|\mathbf{Y} \cdot \mathbf{w} - \mathbf{X} \cdot \mathbf{b}\|^2\}. \tag{2}$$

where $\mathbf{Y}$ is the $N \times T$ Toeplitz output matrix that is given by

$$\mathbf{Y} = \begin{bmatrix} y_{\delta_{tot}} & y_{\delta_{tot}-1} & \cdots & y_{\delta_{tot}-T+1} \\ y_{\delta_{tot}+1} & y_{\delta_{tot}} & \cdots & y_{\delta_{tot}-T+2} \\ \vdots & \vdots & \ddots & \vdots \\ y_{\delta_{tot}+N-1} & y_{\delta_{tot}+N-2} & \cdots & y_{\delta_{tot}-T+N} \end{bmatrix} \quad (3)$$

and $\mathbf{X}$ is the $N \times (v+1)$ Toeplitz input matrix given by

$$\mathbf{X} = \begin{bmatrix} x_0 & x_{-1} & \cdots & x_{-v} \\ x_1 & x_0 & \cdots & x_{-v+1} \\ \vdots & \vdots & \ddots & \vdots \\ x_{N-1} & x_{N-2} & \cdots & x_{N-1-v} \end{bmatrix}. \quad (4)$$

Since we are interested in minimizing this cost function only over the used tones, we will modify the cost function by moving to the frequency domain. We then obtain

$$J = \mathscr{E}\{\|\tilde{\mathbf{Y}} \cdot \mathbf{w} - \tilde{\mathbf{X}} \cdot \mathbf{b}\|^2\}, \quad (5)$$

where

$$\tilde{\mathbf{Y}} = \mathbf{S} \cdot \mathscr{F}_N \cdot \mathbf{Y}, \quad (6)$$

$$\tilde{\mathbf{X}} = \mathbf{S} \cdot \mathscr{F}_N \cdot \mathbf{X}, \quad (7)$$

with $\mathscr{F}_N$ the N-point DFT matrix, and $\mathbf{S}$ the $N \times N$ selection matrix that selects the used tones, i.e., $\mathbf{S}$ is an $N \times N$ diagonal matrix with ones on the positions corresponding to the used tones and zeros elsewhere. Note that if a QAM symbol is modulated on tone i, $i = 2, \ldots, N/2$, the complex conjugated QAM symbol is modulated on tone $N - i + 2$, in order to obtain a real output. Hence, if tone i, $i = 2, \ldots, N/2$, is used, then also tone $N - i + 2$ is used. This means we have $\mathbf{S}(i,i) = \mathbf{S}(N-i+2, N-i+2)$, $i = 2, \ldots, N/2$.

Let us now write the output signal y_l as a function of the input signal x_l and the additive channel noise n_l

$$\mathbf{Y} = \mathbf{X}_{ext}\mathbf{H} + \mathbf{N}, \quad (8)$$

where $\mathbf{N}$ is the $N \times T$ Toeplitz noise matrix that is given by

$$\mathbf{N} = \begin{bmatrix} n_{\delta_{tot}} & n_{\delta_{tot}-1} & \cdots & n_{\delta_{tot}-T+1} \\ n_{\delta_{tot}+1} & n_{\delta_{tot}} & \cdots & n_{\delta_{tot}-T+2} \\ \vdots & \vdots & \ddots & \vdots \\ n_{\delta_{tot}+N-1} & n_{\delta_{tot}+N-2} & \cdots & n_{\delta_{tot}-T+N} \end{bmatrix}, \quad (9)$$

$\mathbf{X}_{ext}$ is the $N \times (L+T)$ Toeplitz extended input matrix given by

$$\mathbf{X}_{ext} = \begin{bmatrix} x_{\delta_{tot}} & x_{\delta_{tot}-1} & \cdots & x_{\delta_{tot}-L-T+1} \\ x_{\delta_{tot}+1} & x_{\delta_{tot}} & \cdots & x_{\delta_{tot}-L-T+2} \\ \vdots & \vdots & \ddots & \vdots \\ x_{\delta_{tot}+N-1} & x_{\delta_{tot}+N-2} & \cdots & x_{\delta_{tot}-L-T+N} \end{bmatrix} \quad (10)$$

and $\mathbf{H}$ is the $(L+T)\times T$ Toeplitz channel matrix given by

$$\mathbf{H} = \begin{bmatrix} \boxed{\mathbf{h}^{\mathrm{T}}} & 0 & \cdots & 0 \\ 0 & \boxed{\mathbf{h}^{\mathrm{T}}} & 0 & \cdots \\ \vdots & \ddots & \ddots & \ddots & \vdots \\ 0 & \cdots & 0 & \boxed{\mathbf{h}^{\mathrm{T}}} \end{bmatrix}^{\mathrm{T}}. \tag{11}$$

Note that $\mathbf{X}_{\mathrm{ext}}$ can be viewed as an extension of $\mathbf{X}$: $\mathbf{X} = \mathbf{X}_{\mathrm{ext}}(:, \delta_{\mathrm{tot}}+1 : \delta_{\mathrm{tot}}+v+1)$. Using (8), the cost function (5) can be rewritten as

$$J = \mathcal{E}\left\{\left\| \left[\, \tilde{\mathbf{X}}_{\mathrm{ext}} \;\middle|\; \tilde{\mathbf{N}} \,\right] \cdot \left[\begin{array}{c|c} \mathbf{H} & \begin{array}{c} \mathbf{0}_{\delta_{\mathrm{tot}}\times(\nu+1)} \\ \hline \mathbf{I}_{\nu+1} \\ \hline \mathbf{0}_{(L+T-\delta_{\mathrm{tot}}-\nu-1)\times(\nu+1)} \end{array} \\ \hline \mathbf{I}_T & \mathbf{0}_{T\times(\nu+1)} \end{array}\right] \cdot \left[\begin{array}{c} \mathbf{w} \\ \hline -\mathbf{b} \end{array}\right] \right\|^2\right\}, \tag{12}$$

where

$$\tilde{\mathbf{N}} = \mathbf{S}\cdot\mathscr{F}_N\cdot\mathbf{N}, \tag{13}$$

$$\tilde{\mathbf{X}}_{\mathrm{ext}} = \mathbf{S}\cdot\mathscr{F}_N\cdot\mathbf{X}_{\mathrm{ext}}. \tag{14}$$

Finally, minimizing (12) can be reformulated as the following MMSE problem:

$$\min_{\mathbf{w},\mathbf{b}} \left\| \left[\begin{array}{c|c} \mathbf{R}^{1/2}_{\tilde{\mathbf{X}}_{\mathrm{ext}}} & \mathbf{0}_{(L+T)\times T} \\ \hline \mathbf{0}_{T\times(L+T)} & \mathbf{R}^{1/2}_{\tilde{\mathbf{N}}} \end{array}\right] \cdot \left[\begin{array}{c|c} \mathbf{H} & \begin{array}{c} \mathbf{0}_{\delta_{\mathrm{tot}}\times(\nu+1)} \\ \hline \mathbf{I}_{\nu+1} \\ \hline \mathbf{0}_{(L+T-\delta_{\mathrm{tot}}-\nu-1)\times(\nu+1)} \end{array} \\ \hline \mathbf{I}_T & \mathbf{0}_{T\times(\nu+1)} \end{array}\right] \cdot \left[\begin{array}{c} \mathbf{w} \\ \hline -\mathbf{b} \end{array}\right] \right\|^2, \tag{15}$$

where $\mathbf{R}_{\tilde{\mathbf{X}}_{\mathrm{ext}}}$ is the extended input correlation matrix $\mathbf{R}_{\tilde{\mathbf{X}}_{\mathrm{ext}}} = \mathscr{E}\{\tilde{\mathbf{X}}^{\mathrm{H}}_{\mathrm{ext}}\cdot\tilde{\mathbf{X}}_{\mathrm{ext}}\}$, and $\mathbf{R}_{\tilde{\mathbf{N}}}$ is the noise correlation matrix: $\mathbf{R}_{\tilde{\mathbf{N}}} = \mathscr{E}\{\tilde{\mathbf{N}}^{\mathrm{H}}\cdot\tilde{\mathbf{N}}\}$.

3.2. Non-triviality constraint

As already mentioned, many constraints can be considered, such as a unit norm, unit tap, or unit output energy constraint on either **w** or **b**. It has been shown that a unit output energy constraint on **w** or **b**, or even on both, all result in the same TEQ **w** (up to a possible scaling), and generally lead to the best performance in terms of bit rate [17]. Here, we consider a unit output energy constraint on **b**

$$\mathscr{E}\{\|\mathbf{X}\cdot\mathbf{b}\|^2\} = 1.$$

As we did for the cost function, we adapt this constraint by disregarding the unused tones

$$\mathscr{E}\{\|\tilde{\mathbf{X}}\cdot\mathbf{b}\|^2\} = 1, \tag{16}$$

which can be written as

$$\mathscr{E}\{\mathbf{b}^{\mathrm{H}} \cdot \mathbf{X}^{\mathrm{H}} \cdot \mathscr{F}_N^{\mathrm{H}} \cdot \mathbf{S} \cdot \mathscr{F}_N \cdot \mathbf{X} \cdot \mathbf{b}\} = 1, \tag{17}$$

where we will explicitly take the cyclic prefix and the unused tones into account for the matrix $\mathbf{X}$. First of all, it is clear that we can rewrite $\mathbf{X} \cdot \mathbf{b}$ as $\mathbf{X}_{\mathrm{circ}} \cdot \mathbf{b}_{\mathrm{zp}}$, where $\mathbf{X}_{\mathrm{circ}}$ is an $N \times N$ matrix that is obtained by circularly extending $\mathbf{X}$, and $\mathbf{b}_{\mathrm{zp}}$ is an $N \times 1$ vector that is obtained by zero-padding $\mathbf{b}$. The non-triviality constraint can then be written as

$$\mathscr{E}\{\mathbf{b}_{\mathrm{zp}}^{\mathrm{H}} \cdot \mathbf{X}_{\mathrm{circ}}^{\mathrm{H}} \cdot \mathscr{F}_N^{\mathrm{H}} \cdot \mathbf{S} \cdot \mathscr{F}_N \cdot \mathbf{X}_{\mathrm{circ}} \cdot \mathbf{b}_{\mathrm{zp}}\} = 1. \tag{18}$$

After the insertion of $(1/N \cdot \mathscr{F}_N^{\mathrm{H}}) \cdot \mathscr{F}_N = \mathbf{I}_N$ between $\mathbf{b}_{\mathrm{zp}}^{\mathrm{H}}$ and $\mathbf{X}_{\mathrm{circ}}^{\mathrm{H}}$ and between $\mathbf{X}_{\mathrm{circ}}$ and $\mathbf{b}_{\mathrm{zp}}$, and using the fact that a circulant matrix is diagonalized by means of DFT matrices, we obtain

$$\mathscr{E}\{\tilde{\mathbf{b}}^{\mathrm{H}} \cdot \mathrm{diag}\{\tilde{\mathbf{x}}\}^{\mathrm{H}} \cdot \mathbf{S} \cdot \mathrm{diag}\{\tilde{\mathbf{x}}\} \cdot \tilde{\mathbf{b}}\} = 1, \tag{19}$$

where the $N \times 1$ vector $\tilde{\mathbf{b}}$ is the DFT of the $N \times 1$ vector $\mathbf{b}_{\mathrm{zp}}$: $\tilde{\mathbf{b}} = \mathscr{F}_N \cdot \mathbf{b}_{\mathrm{zp}}$, and the $N \times 1$ vector $\tilde{\mathbf{x}}$ is the DFT of the $N \times 1$ vector $\mathbf{X}_{\mathrm{circ}}(:,1)$: $\tilde{\mathbf{x}} = \mathscr{F}_N \cdot \mathbf{X}_{\mathrm{circ}}(:,1)$. In other words, the non-triviality constraint becomes

$$\sum_{i=\text{used tone}} |\tilde{b}_i|^2 \cdot \mathscr{E}\{|\tilde{x}_i|^2\} = 1, \tag{20}$$

where $\tilde{b}_i$ and $\tilde{x}_i$ are the ith elements of $\tilde{\mathbf{b}}$ and $\tilde{\mathbf{x}}$, respectively. They denote the TIR and the QAM symbol on the ith tone, respectively. It is further assumed that $\mathscr{E}\{|\tilde{x}_i|^2\}$ is constant for the used tones: $\mathscr{E}\{|\tilde{x}_i|^2\} = P$, $i =$ used tone. As a result, the non-triviality constraint can be rewritten as

$$\begin{aligned}\tilde{\mathbf{b}}^{\mathrm{H}} \cdot \mathbf{S} \cdot \tilde{\mathbf{b}} &= \mathbf{b}_{\mathrm{zp}}^{\mathrm{H}} \cdot \mathscr{F}_N^{\mathrm{H}} \cdot \mathbf{S} \cdot \mathscr{F}_N \cdot \mathbf{b}_{\mathrm{zp}} \\ &= \mathbf{b}^{\mathrm{H}} \cdot \mathbf{R}^{\mathrm{H}} \cdot \mathbf{Q}^{\mathrm{H}} \cdot \mathbf{Q} \cdot \mathbf{R} \cdot \mathbf{b} \\ &= \mathbf{b}^{\mathrm{H}} \cdot \mathbf{R}^{\mathrm{H}} \cdot \mathbf{R} \cdot \mathbf{b} = 1/P,\end{aligned} \tag{21}$$

where $\mathbf{Q} \cdot \mathbf{R}$ is the QR decomposition of $\mathbf{S} \cdot \mathscr{F}_N(:, 1 : v+1)$. With $\mathbf{c} = \mathbf{R} \cdot \mathbf{b}$, the minimization problem then becomes

$$\min_{\mathbf{w},\mathbf{c}} \left\| \left[\begin{array}{c|c} \mathbf{R}_{\tilde{\mathbf{X}}_{\mathrm{ext}}}^{1/2} & \mathbf{0}_{(L+T)\times T} \\ \hline \mathbf{0}_{T\times(L+T)} & \mathbf{R}_{\tilde{\mathbf{N}}}^{1/2} \end{array}\right] \cdot \left[\begin{array}{c|c} & \mathbf{0}_{\delta_{\mathrm{tot}}\times(v+1)} \\ \mathbf{H} & \mathbf{I}_{v+1} \\ & \mathbf{0}_{(L+T-\delta_{\mathrm{tot}}-v-1)\times(v+1)} \\ \hline \mathbf{I}_T & \mathbf{0}_{T\times(v+1)} \end{array}\right] \cdot \left[\begin{array}{c|c} \mathbf{I}_T & \mathbf{0}_{T\times(v+1)} \\ \hline \mathbf{0}_{(v+1)\times T} & \mathbf{R}^{-1} \end{array}\right] \cdot \left[\begin{array}{c} \mathbf{w} \\ \hline -\mathbf{c} \end{array}\right] \right\|^2, \tag{22}$$

subject to $\mathbf{c}^{\mathrm{H}} \cdot \mathbf{c} = 1/P$. The effect of the constant P is only a scaling of the unit norm solution for $\mathbf{c}$ by $1/\sqrt{[]}P$, and thus $\mathbf{b}$ and $\mathbf{w}$ are also scaled by $1/\sqrt{[]}P$. As a scaling of the TEQ $\mathbf{w}$ does not alter the SNR on the tones, and hence the bit rate of the DMT system, the constant P can without loss of generality be set to 1. Defining the $(L+2T) \times (T+v+1)$ matrix $\mathbf{A}$ as

$$\mathbf{A} = \left[\begin{array}{c|c} \mathbf{R}_{\tilde{\mathbf{X}}_{\mathrm{ext}}}^{1/2} & \mathbf{0}_{(L+T)\times T} \\ \hline \mathbf{0}_{T\times(L+T)} & \mathbf{R}_{\tilde{\mathbf{N}}}^{1/2} \end{array}\right] \cdot \left[\begin{array}{c|c} & \mathbf{0}_{\delta_{\mathrm{tot}}\times(v+1)} \\ \mathbf{H} & \mathbf{I}_{v+1} \\ & \mathbf{0}_{(L+T-\delta_{\mathrm{tot}}-v-1)\times(v+1)} \\ \hline \mathbf{I}_T & \mathbf{0}_{T\times(v+1)} \end{array}\right] \cdot \left[\begin{array}{c|c} \mathbf{I}_T & \mathbf{0}_{T\times(v+1)} \\ \hline \mathbf{0}_{(v+1)\times T} & \mathbf{R}^{-1} \end{array}\right]$$

and computing its QR decomposition: $\mathbf{A} = \mathbf{Q}_A \cdot \mathbf{R}_A$, we can then rewrite the constrained MMSE problem (22) as

$$\min_{\mathbf{w},\mathbf{c}} \left\| \mathbf{R}_A \cdot \left[\begin{array}{c} \mathbf{w} \\ \hline -\mathbf{c} \end{array} \right] \right\|^2,$$

subject to $\mathbf{c}^{\mathrm{H}} \cdot \mathbf{c} = 1$. Since $\mathbf{R}_A$ is upper triangular, this can be rewritten as

$$\min_{\mathbf{w},\mathbf{c}} \{ \| \mathbf{R}_A(1:T, 1:T) \cdot \mathbf{w} - \mathbf{R}_A(1:T, T+1:T+v+1) \cdot \mathbf{c} \|^2 + \| \mathbf{R}_A(T+1:T+v+1, T+1:T+v+1) \cdot \mathbf{c} \|^2 \}, \tag{23}$$

subject to $\mathbf{c}^{\mathrm{H}} \cdot \mathbf{c} = 1$. If $\mathbf{R}_A(1:T, 1:T)$ is invertible, the first term can always be set to zero. We therefore start by solving

$$\min_{\mathbf{c}} \| \mathbf{R}_A(T+1:T+v+1, T+1:T+v+1) \cdot \mathbf{c} \|^2$$

subject to $\mathbf{c}^{\mathrm{H}} \cdot \mathbf{c} = 1$. The solution is given by the right singular vector of $\mathbf{R}_A(T+1:T+v+1, T+1:T+v+1)$ corresponding to the smallest singular value. Hence, we first compute the singular value decomposition of $\mathbf{R}_A(T+1:T+v+1, T+1:T+v+1)$: $\mathbf{R}_A(T+1:T+v+1, T+1:T+v+1) = \mathbf{U} \cdot \mathbf{\Sigma} \cdot \mathbf{V}^{\mathrm{H}}$, and then take $\mathbf{c}_{\mathrm{opt}} = \mathbf{V}(:, v+1)$. The first term in (23) is finally set to zero by taking $\mathbf{w}_{\mathrm{opt}} = \mathbf{R}_A(1:T, 1:T)^{-1} \cdot \mathbf{R}_A(1:T, T+1:T+v+1) \cdot \mathbf{c}_{\mathrm{opt}}$.

3.3. Interpretation

In this section, we interpret the constrained MMSE problem (22), showing that the adopted non-triviality constraint is meaningful. From (5) and (16), it is clear that the solution of the constrained MMSE problem is equal to the solution of the following unconstrained MMSE problem (up to a scaling ambiguity):

$$\min_{\mathbf{w},\mathbf{b}} \frac{\left[\begin{array}{c|c} \mathbf{w}^{\mathrm{H}} & -\mathbf{b}^{\mathrm{H}} \end{array} \right] \cdot \left[\begin{array}{c|c} \mathbf{R}_{\tilde{\mathbf{Y}}} & \tilde{\mathbf{R}}^{\mathrm{H}}_{\tilde{\mathbf{X}}\tilde{\mathbf{Y}}} \\ \hline \mathbf{R}_{\tilde{\mathbf{X}}\tilde{\mathbf{Y}}} & \mathbf{R}_{\tilde{\mathbf{X}}} \end{array} \right] \cdot \left[\begin{array}{c} \mathbf{w} \\ \hline -\mathbf{b} \end{array} \right]}{\mathbf{b}^{\mathrm{H}} \cdot \mathbf{R}_{\tilde{\mathbf{X}}} \cdot \mathbf{b}}, \tag{24}$$

where $\mathbf{R}_{\tilde{\mathbf{X}}}$ is the input correlation matrix $\mathbf{R}_{\tilde{\mathbf{X}}} = \mathscr{E}\{\tilde{\mathbf{X}}^{\mathrm{H}} \cdot \tilde{\mathbf{X}}\}$, $\mathbf{R}_{\tilde{\mathbf{Y}}}$ is the output correlation matrix: $\mathbf{R}_{\tilde{\mathbf{Y}}} = \mathscr{E}\{\tilde{\mathbf{Y}}^{\mathrm{H}} \cdot \tilde{\mathbf{Y}}\}$, and $\mathbf{R}_{\tilde{\mathbf{X}}\tilde{\mathbf{Y}}}$ is the input/output crosscorrelation matrix: $\mathbf{R}_{\tilde{\mathbf{X}}\tilde{\mathbf{Y}}} = \mathscr{E}\{\tilde{\mathbf{X}}^{\mathrm{H}} \cdot \tilde{\mathbf{Y}}\}$. This can be explained as follows. The solution of the unconstrained MMSE problem (24) is clearly determined up to a scaling ambiguity. If we scale the solution such that the denominator is one, the obtained result must obviously minimize the numerator under the constraint of the denominator being one, and hence leads to the solution of the constrained MMSE problem. The cost function in (24) can be seen as a sort of 1/SNR in the subband of the used tones. For every value of subband signal energy in the denominator, the subband MSE in the numerator is minimized as shown in Eq. (15), with the subband energy taken as the sum of the energies of the used tones. Note that this optimization criterion does not correspond to the ultimate goal, namely SNR optimization for each tone separately, but it comes close.

3.4. Correlation matrices

To solve the constrained MMSE problem (22), the noise and extended input correlation matrices are needed. These correlation matrices can be written as

$$\mathbf{R}_{\tilde{\mathbf{N}}} = \mathscr{E}\{\tilde{\mathbf{N}}^{\mathrm{H}} \cdot \tilde{\mathbf{N}}\} = \mathscr{E}\{\mathbf{N}^{\mathrm{H}} \cdot \mathscr{F}_N^{\mathrm{H}} \cdot \mathbf{S} \cdot \mathscr{F}_N \cdot \mathbf{N}\}, \tag{25}$$

$$\mathbf{R}_{\tilde{\mathbf{X}}_{\mathrm{ext}}} = \mathscr{E}\{\tilde{\mathbf{X}}_{\mathrm{ext}}^{\mathrm{H}} \cdot \tilde{\mathbf{X}}_{\mathrm{ext}}\} = \mathscr{E}\{\mathbf{X}_{\mathrm{ext}}^{\mathrm{H}} \mathscr{F}_N^{\mathrm{H}} \cdot \mathbf{S} \cdot \mathscr{F}_N \cdot \mathbf{X}_{\mathrm{ext}}\}, \tag{26}$$

where the $\mathbf{S}$ matrix basically selects the appropriate rows and columns in $\mathscr{F}_N$ and $\mathscr{F}_N^{\mathrm{H}}$, respectively. In Appendix A, we prove that the product $\mathscr{F}_N^{\mathrm{H}} \cdot \mathbf{S} \cdot \mathscr{F}_N$ forms an $N \times N$ real symmetric circulant weight matrix. In other words, we can write

$$\mathscr{F}_N^{\mathrm{H}} \cdot \mathbf{S} \cdot \mathscr{F}_N = \begin{bmatrix} a_1 & a_2 & \cdots & a_{N/2} & a_{N/2+1} & a_{N/2} & \cdots & a_2 \\ a_2 & a_1 & a_2 & \cdots & a_{N/2} & a_{N/2+1} & a_{N/2} & \cdots \\ \vdots & a_2 & a_1 & \ddots & \vdots & \ddots & \ddots & \ddots \\ a_{N/2} & \vdots & \ddots & a_1 & a_2 & \ddots & \ddots & a_{N/2+1} \\ a_{N/2+1} & a_{N/2} & \cdots & a_2 & a_1 & a_2 & \cdots & a_{N/2} \\ a_{N/2} & a_{N/2+1} & \ddots & \ddots & a_2 & a_1 & \ddots & \ddots \\ \vdots & a_{N/2} & \ddots & \ddots & \vdots & \ddots & \ddots & a_2 \\ a_2 & \vdots & \ddots & a_{N/2+1} & a_{N/2} & \ddots & a_2 & a_1 \end{bmatrix}, \tag{27}$$

where $a_1, \ldots, a_{N/2+1} \in \mathbb{R}$. Also shown in Appendix A is that

$$[a_1, a_2, \ldots, a_{N/2}, a_{N/2+1}, a_{N/2}, \ldots, a_2]^{\mathrm{T}} = \mathscr{F}_N \cdot \mathrm{diag}\{\mathbf{S}\}.$$

In Appendix B, we then prove that for white additive channel noise n_l (obtained by ignoring the color due to the receive filters) and a white input signal x_l (obtained by ignoring the color due to the presence of the cyclic prefix and the unused tones), the correlation matrices can be written as

$$\mathbf{R}_{\tilde{\mathbf{N}}} = \mathbf{T}_T \cdot \mathscr{E}\{n_l^2\}, \tag{28}$$

$$\mathbf{R}_{\tilde{\mathbf{X}}_{\mathrm{ext}}} = \mathbf{T}_{L+T} \cdot \mathscr{E}\{x_l^2\}, \tag{29}$$

where $\mathbf{T}_K$ is a $K \times K$ real symmetric Toeplitz matrix, where each diagonal contains the sum of the elements on the corresponding diagonal of the weight matrix of (27), the sum being zero if the weight matrix of (27) does not contain this diagonal (this occurs when $K > N$):

$$\mathbf{T}_K = \begin{bmatrix} N\cdot a_1 & (N-1)\cdot a_2 & \cdots & a_2 & 0 & \cdots & 0 \\ (N-1)\cdot a_2 & N\cdot a_1 & (N-1)\cdot a_2 & \cdots & a_2 & \ddots & \vdots \\ \vdots & (N-1)\cdot a_2 & N\cdot a_1 & \ddots & \ddots & \ddots & 0 \\ a_2 & \vdots & \ddots & \ddots & \ddots & \ddots & a_2 \\ 0 & a_2 & \ddots & \ddots & \ddots & \ddots & \vdots \\ \vdots & \ddots & \ddots & \ddots & \ddots & \ddots & (N-1)\cdot a_2 \\ 0 & \cdots & 0 & a_2 & \cdots & (N-1)\cdot a_2 & N\cdot a_1 \end{bmatrix}. \tag{30}$$

Above, we have assumed that the additive channel noise n_l and the input signal x_l are white. These assumptions simplify the expressions of the required correlation matrices but are not true in practice. In an actual DMT system, the receive filters color the additive channel noise n_l, and the presence of the cyclic prefix and the unused tones color the input signal x_l. We now show how the noise and extended input correlation matrix can be computed by incorporating the color of the noise and input signal. The basic idea is to rewrite the noise and extended input correlation matrices as

$$\begin{aligned} \mathbf{R}_{\tilde{\mathbf{N}}} &= \mathscr{E}\{\mathbf{N}^{\mathrm{H}}\cdot\mathscr{F}_N^{\mathrm{H}}\cdot\mathbf{S}\cdot\mathscr{F}_N\cdot\mathbf{N}\} \\ &= \mathscr{E}\{\mathbf{D}_T^{\mathrm{H}}\cdot(\mathbf{I}_N\otimes\mathbf{n}^*)(\mathbf{I}_N\otimes\mathbf{n}^{\mathrm{T}})\mathbf{D}_T\} \\ &= \mathbf{D}_T^{\mathrm{H}}(\mathbf{I}_N\otimes\mathbf{R}_{\mathbf{n}}^*)\mathbf{D}_T, \end{aligned} \tag{31}$$

$$\begin{aligned} \mathbf{R}_{\tilde{\mathbf{X}}_{\mathrm{ext}}} &= \mathscr{E}\{\mathbf{X}_{\mathrm{ext}}^{\mathrm{H}}\cdot\mathscr{F}_N^{\mathrm{H}}\cdot\mathbf{S}\cdot\mathscr{F}_N\cdot\mathbf{X}_{\mathrm{ext}}\} \\ &= \mathscr{E}\{\mathbf{D}_{L+T}^{\mathrm{H}}\cdot(\mathbf{I}_N\otimes\mathbf{x}^*)(\mathbf{I}_N\otimes\mathbf{x}^{\mathrm{T}})\mathbf{D}_{L+T}\} \\ &= \mathbf{D}_{L+T}^{\mathrm{H}}(\mathbf{I}_N\otimes\mathbf{R}_{\mathbf{x}}^*)\mathbf{D}_{L+T}, \end{aligned} \tag{32}$$

where $\mathbf{n} = [n_{\delta_{\mathrm{tot}}-T+1},\ldots,n_{\delta_{\mathrm{tot}}+N-1}]^{\mathrm{T}}$, $\mathbf{x} = [x_{\delta_{\mathrm{tot}}-L-T+1},\ldots,x_{\delta_{\mathrm{tot}}+N-1}]^{\mathrm{T}}$, $\mathbf{R}_{\mathbf{n}} = \mathscr{E}\{\mathbf{n}\mathbf{n}^{\mathrm{H}}\}$, $\mathbf{R}_{\mathbf{x}} = \mathscr{E}\{\mathbf{x}\mathbf{x}^{\mathrm{H}}\}$, and $\mathbf{D}_t = [\mathbf{D}_{t,i_1}^{\mathrm{T}},\ldots,\mathbf{D}_{t,i_K}^{\mathrm{T}}]^{\mathrm{T}}$, with $i_1,\ldots,i_K$ the used tones and $\mathbf{D}_{t,i}$ the $(N+t-1)\times t$ Hankel matrix given by

$$\mathbf{D}_{t,i} = \begin{bmatrix} 0 & \cdots & 0 & \boxed{\mathcal{F}_N(i,:)} \\ \cdots & 0 & \boxed{\mathcal{F}_N(i,:)} & 0 \\ \vdots & \iddots & \iddots & \iddots & \vdots \\ \boxed{\mathcal{F}_N(i,:)} & 0 & \cdots & 0 \end{bmatrix}^{\mathrm{T}}. \tag{33}$$

It is further convenient to translate $\mathbf{R}_{\mathbf{x}}$ to the frequency domain. Therefore, we rewrite $\mathbf{x}$ as a function of the frequency domain symbols as

$$\mathbf{x} = [\mathbf{0}_{\alpha\times\beta},\mathbf{I}_\alpha,\mathbf{0}_{\alpha\times\gamma}]\cdot(\mathbf{I}_3\otimes 1/N\cdot\mathbf{P}\cdot\mathscr{F}_N^{\mathrm{H}})\cdot[\tilde{\mathbf{x}}_-^{\mathrm{T}},\tilde{\mathbf{x}}^{\mathrm{T}},\tilde{\mathbf{x}}_+^{\mathrm{T}}]^{\mathrm{T}}, \tag{34}$$

where $\alpha = N + L + T - 1$, $\beta = N + 2v + \delta_{\text{tot}} - L - T + 1$, $\gamma = N + v - \delta_{\text{tot}}$, the vectors $\tilde{\mathbf{x}}_{-}$ and $\tilde{\mathbf{x}}_{+}$ are the previous and next DMT symbol, respectively, and the matrix $\mathbf{P}$ represents the matrix that adds a cyclic prefix

$$\mathbf{P} = \left[\begin{array}{c|c} \mathbf{0}_{\nu\times(N-\nu)} & \mathbf{I}_{\nu} \\ \hline \multicolumn{2}{c}{\mathbf{I}_N} \end{array}\right].$$

As a result, we can express $\mathbf{R}_{\mathbf{x}}$ as

$$\mathbf{R}_{\mathbf{x}} = [\mathbf{0}_{\alpha\times\beta}, \mathbf{I}_{\alpha}, \mathbf{0}_{\alpha\times\gamma}] \cdot (\mathbf{I}_3 \otimes 1/N^2 \cdot \mathbf{P} \cdot \mathscr{F}_N^{\mathrm{H}} \cdot \mathbf{R}_{\tilde{\mathbf{x}}} \cdot \mathscr{F}_N \cdot \mathbf{P}^{\mathrm{H}}) \cdot [\mathbf{0}_{\alpha\times\beta}, \mathbf{I}_{\alpha}, \mathbf{0}_{\alpha\times\gamma}]^{\mathrm{T}}. \tag{35}$$

where $\mathbf{R}_{\tilde{\mathbf{x}}} = \mathscr{E}\{\tilde{\mathbf{x}}\tilde{\mathbf{x}}^{\mathrm{H}}\}$.

4. Simulation results

To compare the performance of different equalizers, simulation results are presented for an upstream ADSL channel. We consider a 4 km 26 AWG 'inline' loop, i.e., without bridged taps. Simulation results for other loop lengths and some more difficult reference loops show a similar behavior (see [11, Chapter 3]). The additive channel noise consists of −140 dBm/Hz white Gaussian noise (colored by the receive filters). A frequency division multiplexing (FDM) set-up is adopted and the residual echo is taken into account. The transfer function of the channel and the noise power spectral density (PSD) are obtained from a simulation model from Alcatel. The channel transfer function includes the model of the copper wire itself as well as the digital and analog transmit and receive filters.

To compute the bit rate, we compute the SNR for each used tone i (denoted as SNR_i), and take the SNR gap $\Gamma = 9.8$ dB, noise margin $\gamma_{\mathrm{m}} = 6$ dB, and coding gain $\gamma_{\mathrm{c}} = 3$ dB. The number of bits assigned to tone i is then given by

$$N_i = \left\lfloor \log_2\left(1 + 10\frac{\mathrm{SNR}_i - \Gamma - \gamma_{\mathrm{m}} + \gamma_{\mathrm{c}}}{10}\right)\right\rfloor. \tag{36}$$

The bit rate is computed with the formula

$$R = \left(\sum_{i=\text{used tone}} N_i\right)\frac{F_{\mathrm{S}}}{N + v} \tag{37}$$

with F_{s} the sample rate.

For the simulations, we take DMT symbol size $N = 128$, cyclic prefix length $v = 8$, used tones from 8 to 30, sample rate $F_{\mathrm{s}} = 552$ kHz, and a signal PSD of −38 dBm/Hz.

In Fig. 2, two TEQ algorithms are compared for two TEQ lengths. The first algorithm is the proposed weighted MMSE channel shortening algorithm (denoted by '$\|S \cdot B\| = 1$'), and minimizes the constrained problem (22) assuming colored noise, i.e., using (31), and a white input signal, i.e., using (29). Note that we take only the used tones into account in the non-triviality constraint as well as in the cost function (by the weighting matrix $\mathbf{S}$). The second algorithm is the classical MMSE channel shortening algorithm (denoted by '$\|b\| = 1$'), and basically minimizes the constrained problem (22) without taking into account the used

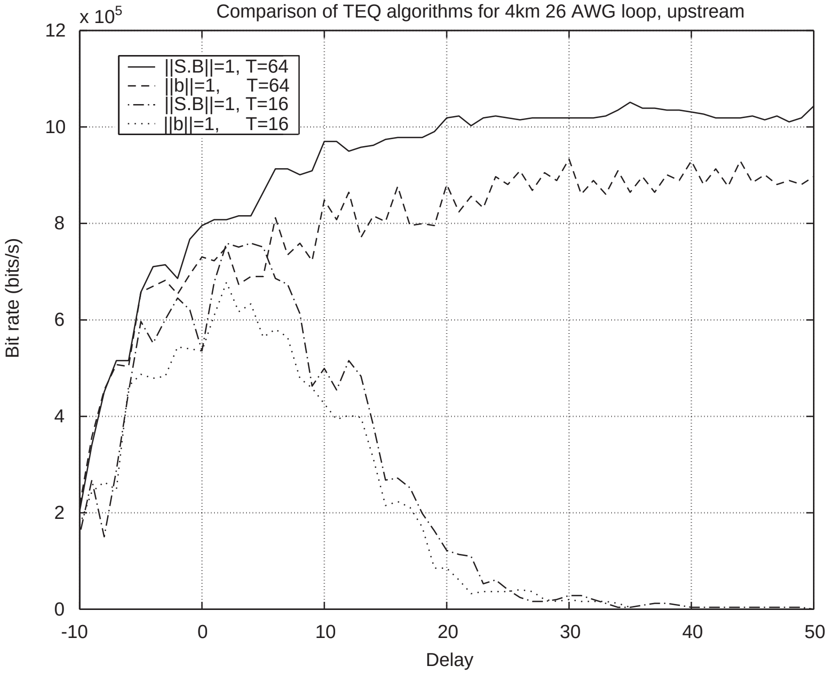

Fig. 2. Comparison of weighted MMSE with classical MMSE channel shortening for a 4 km 26 AWG upstream loop.

tones, i.e., we assume $\mathbf{S} = \mathbf{I}_N$. Note that this means that $\mathbf{R} = \sqrt{[]}N\mathbf{I}_{v+1}$ in (22). Again we assume colored noise, i.e., we use (31) with $\mathbf{S} = \mathbf{I}_N$ (this leads to $\mathbf{R}_{\tilde{\mathbf{N}}} = N^2\mathbf{R}_{\mathbf{n}}(1:T, 1:T)$), and a white input signal, i.e., we use (29) with $\mathbf{S} = \mathbf{I}_N$ (this leads to $\mathbf{R}_{\tilde{\mathbf{X}}_{\text{ext}}} = N^2\mathbf{I}_{L+T} \cdot \mathscr{E}\{x_l^2\}$). Note that except for the fact that a few matrices in (22) become identity for the classical MMSE channel shortening algorithm, there is no major difference in complexity between the two approaches. The considered TEQ lengths are 16 and 64. The weighted MMSE channel shortening algorithm is clearly better than the classical MMSE channel shortening for $T = 64$ and for $T = 16$. The delay dependency is still a problem, but it is clear that when the equalizer length increases, the difference in smoothness between the two approaches also increases. In upstream, a relatively small number of tones is used (only 8 up to 30 of the 65 tones). For this reason, the performance increase with the weighted criterion is more apparent in upstream than in downstream (see [11, Chapter 3]).

5. Conclusions

Existing MMSE channel shortening algorithms do not correspond to bit rate optimization, which is a major disadvantage. In this paper, we have modified the classical MMSE channel shortening algorithm by the introduction of weight matrices in the cost function as well as in the constraint, to explicitly disregard the unused tones. Simplified formulas for the correlation matrices in the case of white noise and input signal are derived. Optimizing the weighted MSE can be seen as minimizing a sort of 1/SNR over the subband of used tones. The weighted MMSE channel shortening shows a significant performance increase in upstream. Note that the modified weighted cost function still does not correspond to bit rate optimization, but it comes close.

Acknowledgements

This research work was supported by the Belgian Programme on Interuniversity Attraction Poles, initiated by the Belgian Federal Science Policy Office IUAP P5/22 ('Dynamical Systems and Control: Computation, Identification and Modelling') and P5/11 ('Mobile multimedia communication systems and networks'), the Concerted Research Action GOA-MEFISTO-666 (Mathematical Engineering for Information and Communication Systems Technology) of the Flemish Government, Research Project FWO nr.G.0196.02 ('Design of Efficient Communication Techniques for Wireless Time-Dispersive Multi-User MIMO Systems'), IWT Project 030054 SOLIDT ('Solutions for xDSL Interoperability, Deployment and New Technologies'), and NWO-STW under the VICI Programme (DTC.5893), and was partially sponsored by Alcatel-Bell.

Appendix A

Property 1. *Suppose* $\mathscr{F}_N$ *is the N-point DFT matrix and* $\mathbf{S}$ *is an* $N \times N$ *selection matrix that selects the used tones, i.e.,* $\mathbf{S}$ *is an* $N \times N$ *diagonal matrix with ones on the positions corresponding to the used tones and zeros elsewhere. Then the matrix* $\mathscr{F}_N^{\mathrm{H}} \cdot \mathbf{S} \cdot \mathscr{F}_N$ *is an* $N \times N$ *real symmetric circulant weight matrix.*

Proof.

- $\mathscr{F}_N^{\mathrm{H}} \cdot \mathbf{S} \cdot \mathscr{F}_N$ is real: The element on the mth row and the nth column is given by

$$\sum_{i=\text{used tone}} \mathrm{e}^{\mathrm{j}2\pi m(i-1)/N} \mathrm{e}^{-\mathrm{j}2\pi(i-1)n/N}$$

$$= \sum_{i=\text{used tone}} \mathrm{e}^{\mathrm{j}2\pi(i-1)(m-n)/N} \tag{A.1}$$

$$= \sum_{\substack{i=\text{used tone}\\ i=2,\ldots,N/2}} \mathrm{e}^{\mathrm{j}2\pi(i-1)(m-n)/N} + \mathrm{e}^{\mathrm{j}2\pi(N-i+1)(m-n)/N} \tag{A.2}$$

$$= \sum_{\substack{i=\text{used tone}\\ i=2,\ldots,N/2}} 2\cos(2\pi(i-1)(m-n)/N), \tag{A.3}$$

  where the second equality is due to the fact that if tone i, $i = 2, \ldots, N/2$, is used, then also tone $N-i+2$ is used. Hence, the element on the mth row and the nth column is real.
- $\mathscr{F}_N^{\mathrm{H}} \cdot \mathbf{S} \cdot \mathscr{F}_N$ is symmetric:

$$(\mathscr{F}_N^{\mathrm{H}} \cdot \mathbf{S} \cdot \mathscr{F}_N)^{\mathrm{H}} = \mathscr{F}_N^{\mathrm{H}} \cdot \mathbf{S}^{\mathrm{H}} \cdot \mathscr{F}_N = \mathscr{F}_N^{\mathrm{H}} \cdot \mathbf{S} \cdot \mathscr{F}_N \tag{A.4}$$

- $\mathscr{F}_N^{\mathrm{H}} \cdot \mathbf{S} \cdot \mathscr{F}_N$ is circulant: Since $\mathscr{F}_N^{\mathrm{H}} \cdot \mathbf{S} \cdot \mathscr{F}_N$ can be diagonalized by DFT matrices:

$$\mathscr{F}_N \cdot (\mathscr{F}_N^{\mathrm{H}} \cdot \mathbf{S} \cdot \mathscr{F}_N) \cdot (1/N \cdot \mathscr{F}_N^{\mathrm{H}}) = \mathbf{S}, \tag{A.5}$$

  the matrix $\mathscr{F}_N^{\mathrm{H}} \cdot \mathbf{S} \cdot \mathscr{F}_N$ is circulant. Moreover, the first column of $\mathscr{F}_N^{\mathrm{H}} \cdot \mathbf{S} \cdot \mathscr{F}_N$ is given by the DFT of the vector on the diagonal, i.e., the first column of $\mathscr{F}_N^{\mathrm{H}} \cdot \mathbf{S} \cdot \mathscr{F}_N$ is given by $\mathscr{F}_N \cdot \mathrm{diag}\{\mathbf{S}\}$. □

Appendix B

Property 2. *For white additive channel noise n_l and a white input signal x_l,* $\mathbf{R}_{\tilde{\mathbf{N}}}$ and $\mathbf{R}_{\tilde{\mathbf{X}}_{\text{ext}}}$ *are given by* (28) *and* (29), *respectively*.

Proof. We give the proof for $\mathbf{R}_{\tilde{\mathbf{N}}}$ (a similar proof holds for $\mathbf{R}_{\tilde{\mathbf{X}}_{\text{ext}}}$). Consider the element on the mth row and the nth column of $\mathbf{R}_{\tilde{\mathbf{N}}}$:

$$\mathbf{R}_{\tilde{\mathbf{N}}}(m,n) = \mathscr{E}\{\mathbf{N}(:,m)^{\text{H}} \cdot \mathscr{F}_N^{\text{H}} \cdot \mathbf{S} \cdot \mathscr{F}_N \cdot \mathbf{N}(:,n)\}. \tag{B.1}$$

Suppose $m \leqslant n$ (a similar derivation holds for $m > n$). If $n - m \geqslant N$, the mth and nth column of $\mathbf{N}$ have no common elements. If $n - m < N$, on the other hand, the first $N - (n - m)$ elements of the mth column of $\mathbf{N}$ are equal to the last $N - (n - m)$ elements of the nth column of $\mathbf{N}$. When computing (B.1), only terms that contain a product of two equivalent noise samples have to be considered, due to the fact that the noise is assumed to be white. If $n - m \geqslant N$, it is therefore immediately clear that

$$\mathbf{R}_{\tilde{\mathbf{N}}}(m,n) = 0.$$

If $n - m < N$, on the other hand, the $(n - m)$th diagonal of the matrix $\mathscr{F}_N^{\text{H}} \cdot \mathbf{S} \cdot \mathscr{F}_N$ will come into play. Since $\mathscr{F}_N^{\text{H}} \cdot \mathbf{S} \cdot \mathscr{F}_N$ is circulant, this $(n - m)$th diagonal contains $N - (n - m)$ times the element $a_{(n-m)+1}$ if $n - m = 0, \ldots, N/2$ or $N - (n - m)$ times the element $a_{N+1-(n-m)}$ if $n - m = N/2 + 1, \ldots, N - 1$. Hence, we then obtain

$$\mathbf{R}_{\tilde{\mathbf{N}}}(m,n) = \begin{cases} a_{(n-m)+1}(N - (n - m))\mathscr{E}\{n_l^2\} & \text{if} \quad n - m = 0, \ldots, N/2, \\ a_{N+1-(n-m)}(N - (n - m))\mathscr{E}\{n_l^2\} & \text{if } n - m = N/2 + 1, \ldots, N - 1. \end{cases}$$

References

[1] N. Al-Dhahir, J.M. Cioffi, Optimum finite-length equalization for multicarrier transceivers, IEEE Trans. Comm. 44 (1) (January 1996) 56–64.

[2] N. Al-Dhahir, J.M. Cioffi, Efficiently computed reduced-parameter input-aided MMSE equalizers for ML detection: a unified approach, Trans. Inform. Theory 42 (3) (May 1996) 903–915.

[3] J.S. Chow, J.M. Cioffi, A cost-effective maximum likelihood receiver for multicarrier systems, in: Proceedings of the International Conference on Communication (ICC), Chicago, June 1992, pp. 948–952.

[4] J.S. Chow, J.M. Cioffi, J.A.C. Bingham, Equalizer training algorithms for multicarrier modulation systems, in: Proceedings of the International Conference on Communication (ICC), Geneva, May 1993, pp. 761–765.

[5] J.S. Chow, J.C. Tu, J.M. Cioffi, A discrete multitone transceiver system for HDSL applications, IEEE J. Sel. Areas Comm. 9 (6) (August 1991) 895–908.

[6] I. Lee, J.S. Chow, J.M. Cioffi, Performance evaluation of a fast computation algorithm for the DMT in high-speed subscriber loop, IEEE J. Sel. Areas Comm. 13 (9) (December 1995) 1564–1570.

[7] P.J.W. Melsa, R.C. Younce, C.E. Rohrs, Impulse response shortening for discrete multitone transceivers, IEEE Trans. Comm. 44 (12) (December 1996) 1662–1672.

[8] M. Nafie, A. Gatherer, Time-domain equalizer training for ADSL, in: Proceedings of the International Conference on Communication (ICC), Montreal, Canada, June 1997, pp. 1085–1089.

[9] T. Pollet, M. Peeters, M. Moonen, L. Vandendorpe, Equalization for DMT-based broadband modems, IEEE Comm. Mag. 38 (5) (May 2000) 106–113.

[10] T. Pollet, H. Steendam, M. Moeneclaey, Performance degradation of multicarrier systems caused by an insufficient guard interval, in: Proceedings of the International Workshop on Copper Wire Access Systems, Budapest, Hungary, October 1997, pp. 265–270.

[11] K. Van Acker, Equalization and echo cancellation for DMT-based DSL modems, Ph.D. Thesis, Faculty of Applied Sciences, K.U. Leuven, Leuven, Belgium, January 2001.

[12] K. Van Acker, G. Leus, M. Moonen, O. van de Wiel, T. Pollet, Per tone equalization for DMT-based systems, IEEE Trans. on Commun. 49 (1) (January 2001) 109–119.

[13] M. Van Bladel, M. Moeneclaey, Time-domain equalization for multicarrier communication, in: Proceedings of the IEEE Global Telecommunication Conference (GLOBECOM), Singapore, November 1995, pp. 167–171.
[14] J.-F. Van Kerckhove, P. Spruyt, Adapted optimization criterion for FDM-based DMT-ADSL equalization, in: Proceedings of the International Conference on Communication (ICC), Dallas, TX, June 1996, pp. 1328–1334.
[15] B. Wang, T. Adali, A frequency-domain eigenfilter approach for equalization in discrete multitone systems, in: Proceedings of the Asilomar Conference on Signals, Systems and Computers, Pacific Grove, CA, October 1999, pp. 1058–1062.
[16] B. Wang, T. Adali, Joint impulse response shortening for discrete multitone systems, in: Proceedings of the IEEE Global Telecommunication Conference (GLOBECOM), Rio de Janeiro, Brazil, December 1999, pp. 2508–2512.
[17] G. Ysebaert, K. Van Acker, M. Moonen, B. De Moor, Constraints in channel shortening equalizer design for DMT-based systems, Elsevier Signal Process. 83 (3) (March 2003) 641–648.